Tokyo Climate Center, Japan Meteorological Agency

TCC News

Autumn 2019

Table of Contents: TCC News No. 58

TCC climate monitoring activity on stratospheric circulation in the Northern Hemisphere

The Japan Meteorological Agency (JMA) has long monitored stratospheric sudden warming (SSW) in the Northern Hemisphere during boreal winter, and began providing related information under the STRATALERT program of the World Meteorological Organization (WMO) in the International Year of the Quiet Sun (IQSY) of 1964 – 1965 (e.g., WMO 1964; Labitzke 2005; Butler et al. 2015). The Stratospheric Research Group of the Freie Universität Berlin, Germany, terminated its decades of significant active contributions to the program via STRATALERT report issuance in 2004 (Labitzke 2005), while JMA continued its report provision via the Global Telecommunication System (GTS) on a daily basis in relation to SSW events in the Northern Hemisphere during winter.

In winter 2019/2020, TCC/JMA began issuing Northern Hemisphere SSW monitoring information on the TCC website (https://ds.data.jma.go.jp/tcc/tcc/products/clisys/STRAT/index.html; see criteria). The information are updated whenever a SSW event starts or ends in the Northern Hemisphere and when events are recognized as major SSW instances. It can be accessed along with graphs and maps, including time-series representations of temperature at 30 hPa over the North Pole (Fig. 1-1) updated on a daily basis.

It should be noted that JMA discontinued its GTS issuance of STRATALERT Tokyo reports in November 2019, making winter 2018/2019 the final season of provision. Users' support for STRATALERT Tokyo reports over the years is very much appreciated. TCC expects its future online provision of Northern Hemisphere SSW monitoring information to enhance climate monitoring and seasonal prediction by National Meteorological and Hydrological Services (NMHSs).

(Akihiko Shimpo, Tokyo Climate Center)

References

Butler, A. H., D. J. Seidel, S. C. Hardiman, N. Butchart, T. Birner, and A. Match, 2015: Defining sudden stratospheric warmings. *Bull. Amer. Meteor. Soc.*, **96**, 1913-1928.

Labitzke, K., 2005: Termination of the STRATALERT Reports. *SPARC Newsletter*, **24**, World Climate Research Programme SPARC Office (Available online at http://www.atmosp.physics.utoronto.ca/SPARC/Newsletter%2024%20WEB%20/Stratalert.html, accessed 13 November 2019)

WMO, 1964: Implementation of the WMO-IQSY STRATWARM PROGRAMME. *WMO Bulletin*, **13(4)**, 200-205 (Available online at https://library.wmo.int/doc_num.php?explnum_id=6525, accessed 13 November 2019).

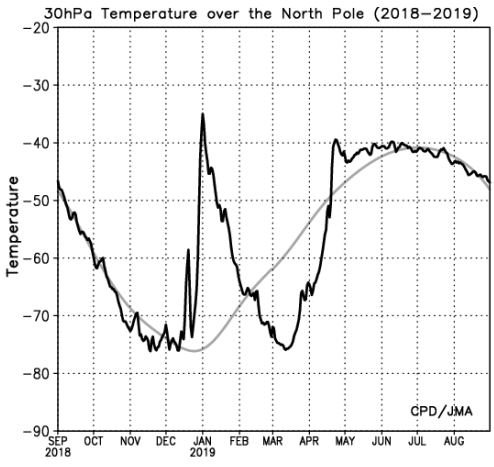

Figure 1-1 Time-series representation of 30-hPa temperature over the North Pole from September 2018 to August 2019. Black line: daily temperature; grey line: normal (1981 – 2010 average).

El Niño Outlook (November 2019 - May 2020)

ENSO-neutral conditions persisted in October 2019, and ENSO-neutral conditions are likely (60%) to continue until boreal spring. (Article based on the El Niño outlook issued on 11 November 2019.)

El Niño/La Niña

The NINO.3 SST deviation was +0.2°C in October. SSTs were above normal in the western part of the equatorial Pacific and near normal in the eastern part (Figures 2-1 and 2-3 (a)), and subsurface temperatures were above normal in the central part (Figures 2-2 and 2-3 (b)). Atmospheric convective activity near the dateline over the equatorial Pacific was near normal, as were easterly winds in the lower troposphere (i.e., trade winds) over the central equatorial Pacific. These oceanic and atmospheric conditions indicate that ENSO-neutral conditions persisted in October.

Since subsurface ocean temperature anomalies in the equatorial Pacific were small, near-normal SST conditions in the eastern part are expected to continue in the coming months. JMA's El Niño prediction model suggests that the NINO.3 SST will be near normal until boreal spring (Figure 2-4). Based on this prediction and the observations detailed above, there is a probability of over 60% that the five-month running mean NINO.3 SST will be between -0.4 and +0.4°C in boreal winter and beyond (Figure 2-5). In conclusion, ENSO-neutral conditions are likely (60%) to continue until boreal spring.

Western Pacific and Indian Ocean

The area-averaged SST in the tropical western Pacific (NINO.WEST) region was near normal in October. Values are likely to be near or below normal until boreal winter and near or above normal in boreal spring.

The area-averaged SST in the tropical Indian Ocean (IOBW) region was above normal in October. Values are likely to be near or above normal until boreal spring.

(Hiroyuki Sugimoto, Tokyo Climate Center)

* The SST normal for the NINO.3 region (5°S – 5°N, 150°W – 90°W) is defined as an monthly average over the latest sliding 30-year period (1989-2018 for this year).
* The SST normals for the NINO.WEST region (Eq. – 15°N, 130°E – 150°E) and the IOBW region (20°S – 20°N, 40°E – 100°E) are defined as linear extrapolations with respect to the latest sliding 30-year period, in order to remove the effects of significant long-term warming trends observed in these regions.

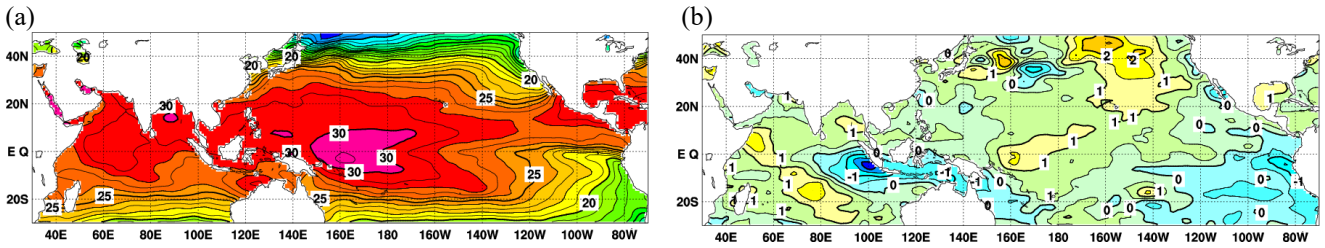

Figure 2-1 Monthly mean (a) sea surface temperatures (SSTs) and (b) SST anomalies in the Indian and Pacific Ocean areas for October 2019

The contour intervals are 1˚C in (a) and 0.5˚C in (b). The base period for the normal is 1981 – 2010.

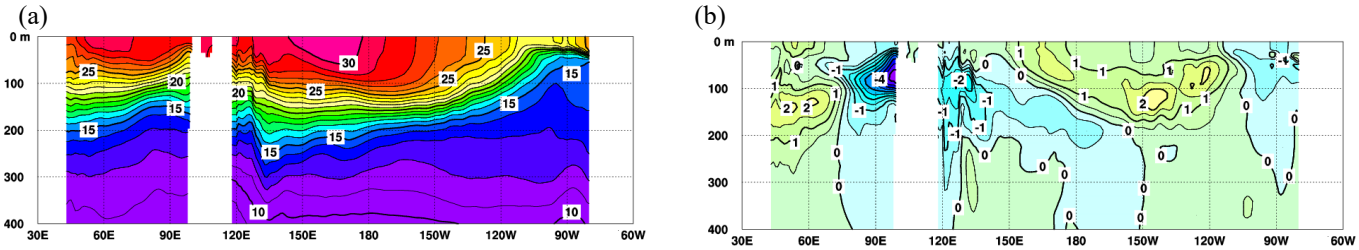

Figure 2-2 Monthly mean depth-longitude cross sections of (a) temperatures and (b) temperature anomalies in the equatorial Indian and Pacific Ocean areas for October 2019

The contour intervals are 1˚C in (a) and 0.5˚C in (b). The base period for the normal is 1981 – 2010.

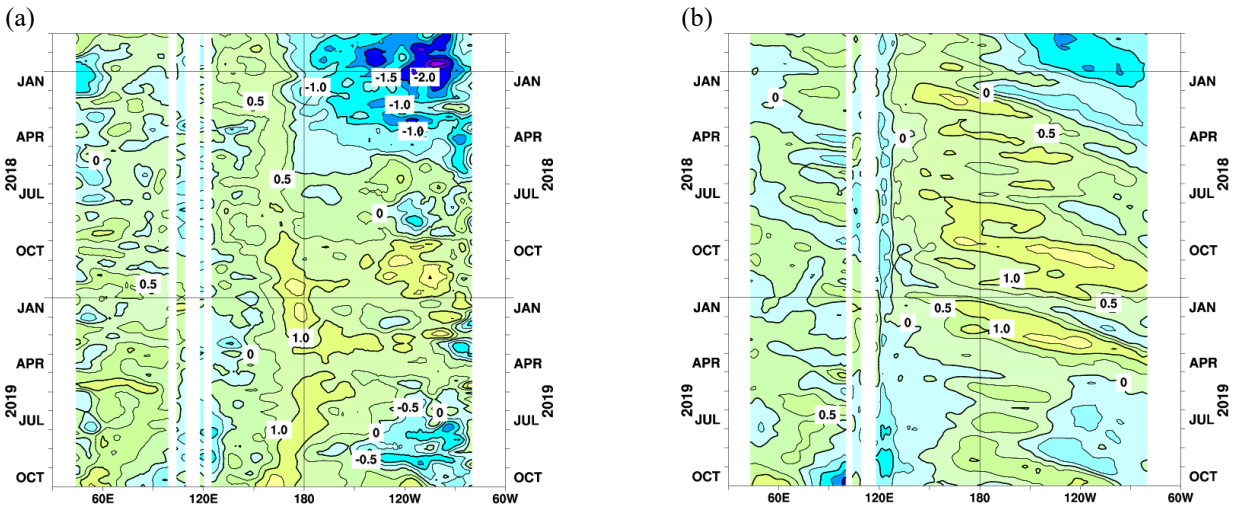

Figure 2-3 Time-longitude cross sections of (a) SST and (b) ocean heat content (OHC) anomalies along the equator in the Indian and Pacific Ocean areas

OHCs are defined here as vertically averaged temperatures in the top 300 m. The base period for the normal is 1981 – 2010.

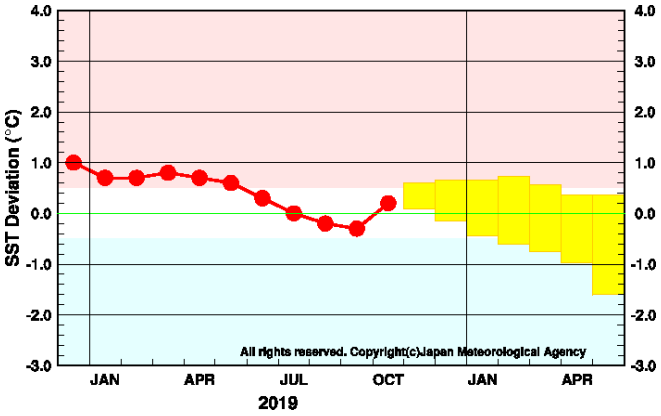

Figure 2-4 Outlook of NINO.3 SST deviation produced by the El Niño prediction model

This figure shows a time series of monthly NINO.3 SST deviations. The thick line with closed circles shows observed SST deviations, and the boxes show the values produced for up to six months ahead by the El Niño prediction model. Each box denotes the range into which the SST deviation is expected to fall with a probability of 70%.

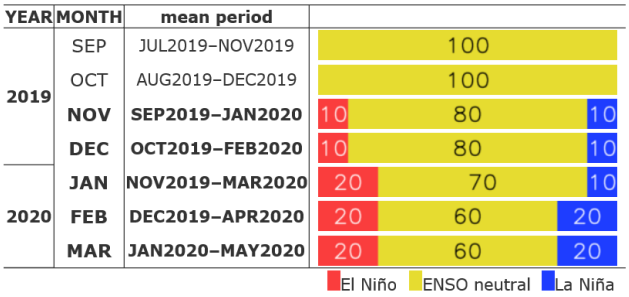

Figure 2-5 ENSO forecast probabilities based on the El Niño prediction model

Red, yellow and blue bars indicate probabilities that the five-month running mean of the NINO.3 SST deviation from the latest sliding 30-year mean will be +0.5°C or above (El Niño), between +0.4 and -0.4°C (ENSO-neutral) and -0.5°C or below (La Niña), respectively. Regular text indicates past months, and bold text indicates current and future months.

<<Table of contents <Top of this article

JMA's Seasonal Numerical Ensemble Prediction for Winter 2019/2020

Based on JMA's seasonal ensemble prediction system, sea surface temperature (SST) anomalies are predicted to be near normal in the equatorial Pacific in boreal winter 2019/2020, suggesting neutral El Niño conditions. In association with remaining Indian Ocean Dipole (IOD) condition, active convection is predicted over the western tropical Indian Ocean (WTIO), while inactive convection is predicted over the south-eastern tropical Indian Ocean (SETIO). As a result, easterly anomalies over the southern tropical Indian Ocean and, in association with the subtropical jet, positive anomalies of the stream function at 200 hPa over Japan are predicted.

1. Introduction

This article outlines JMA's dynamical seasonal ensemble prediction for boreal winter 2019/2020 (December – February, referred to as DJF), which was used as a basis for JMA's operational cold-season outlook issued on 25 November 2019. The outlook is based on the seasonal ensemble prediction system of the Coupled Atmosphere-ocean General Circulation Model (CGCM). See the column below for system details.

Section 2 outlines global SST anomaly predictions, and Section 3 describes the associated circulation field predictions for the tropics and sub-tropics. Finally, the circulation fields predicted for the mid- and high-latitudes of the Northern Hemisphere are discussed in Section 4.

2. SST anomalies (Figure 3-1)

Figure 3-1 shows predicted SSTs (contours) and related anomalies (shading) for DJF. As for SST conditions in the tropical Pacific, near-normal anomalies are predicted in the equatorial Pacific, suggesting neutral El Niño conditions. Meanwhile, above-normal SST conditions are predicted in the southern tropical Indian Ocean under the influence of IOD condition in December and January.

3. Prediction for the tropics and sub-tropics (Figure 3-2)

Figure 3-2 (a) shows predicted precipitation (contours) and related anomalies (shading) for DJF. Above-normal anomalies are predicted over the northern tropical Pacific and the WTIO, while below-normal anomalies are predicted over the SETIO in association with remaining IOD condition.

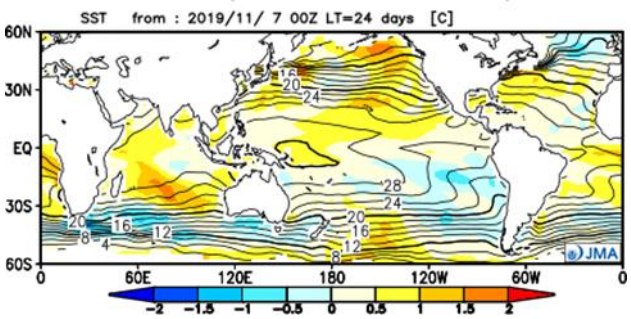

Figure 3-1 Predicted SSTs (contours) and SST anomalies (shading) for December–February 2019/2020 (ensemble mean of 51 members)

(a)

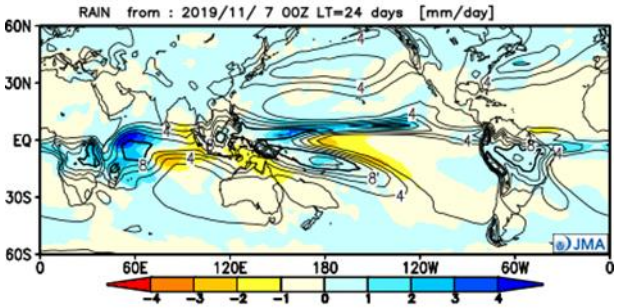

(b)

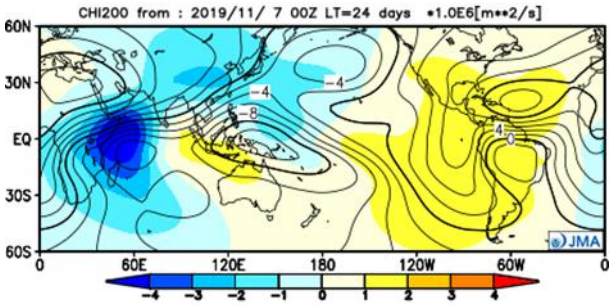

(c)

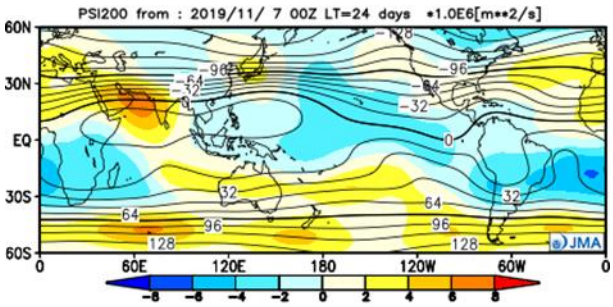

(d)

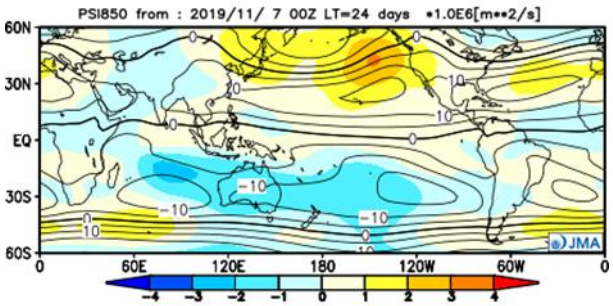

Figure 3-2 Predicted atmospheric fields from 60°N – 60°S for December–February 2019/2020 (ensemble mean of 51 members)

(a) Precipitation (contours) and anomaly (shading). The contour interval is 2 mm/day.

(b) Velocity potential at 200 hPa (contours) and anomaly (shading). The contour interval is 2×10^6 m^2/s.

(c) Stream function at 200 hPa (contours) and anomaly (shading). The contour interval is 16×10^6 m^2/s.

(d) Stream function at 850 hPa (contours) and anomaly (shading). The contour interval is 5×10^6 m^2/s.

Figure 3-2 (b) shows predicted velocity potential (contours) and related anomalies (shading) in the upper troposphere (200 hPa) for DJF. Positive (i.e., convergent) anomalies are predicted over the eastern Indian Ocean in association with inactive convection over the SETIO. Conversely, negative (i.e., divergent) anomalies are predicted over the western Indian Ocean and Africa in association with active precipitation over the WTIO.

Figure 3-2 (c) shows predicted stream functions (contours) and related anomalies (shading) in the upper troposphere (200 hPa) for DJF. Positive (i.e., anticyclonic) anomalies are predicted in the Arabian Sea, in association with divergence over the western Indian Ocean and Africa, which influences through Japan to North America via a Rossby-wave train along the subtropical jet stream.

Figure 3-2 (d) shows predicted stream functions (contours) and related anomalies (shading) in the lower troposphere (850 hPa) for DJF. Equatorial symmetric anticyclonic anomalies are predicted over the Indian Ocean, which generates strong easterly wind anomalies over the southern tropical Indian Ocean. Positive (i.e., anticyclonic) anomalies are seen over sea areas off the western coast of North America and around Japan in association with the barotropic high generated from a Rossby-wave train in the upper troposphere.

4. Prediction for the mid- and high- latitudes of the Northern Hemisphere

Figure 3-3 (a) shows predicted geopotential heights (contours) and related anomalies (shading) at 500 hPa for DJF. Positive anomalies are predicted over the sea off the western coast of North America and around Japan in association with the barotropic high. Conversely, negative anomalies are seen over northern India and central Asia as well as the northern part of America.

Figure 3-3 (b) shows predicted sea level pressure (contours) and related anomalies (shading) for DJF. Positive Arctic Oscillation is predicted to be dominant in the Northern Hemisphere, but this should be interpreted with caution due to low predictability. Positive anomalies are predicted over the sea off the western coast of North America and around Japan in association with the barotropic high.

(a)

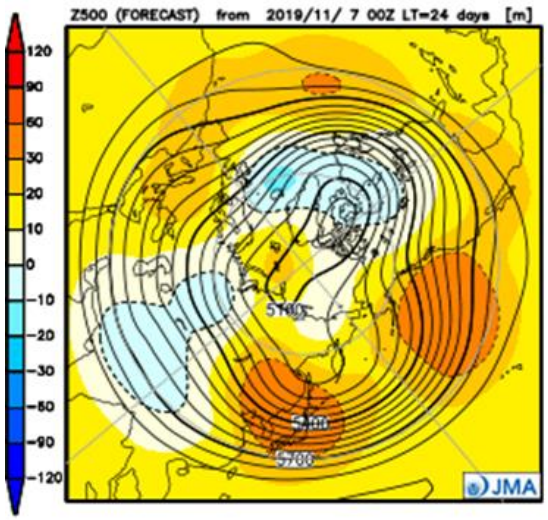

(b)

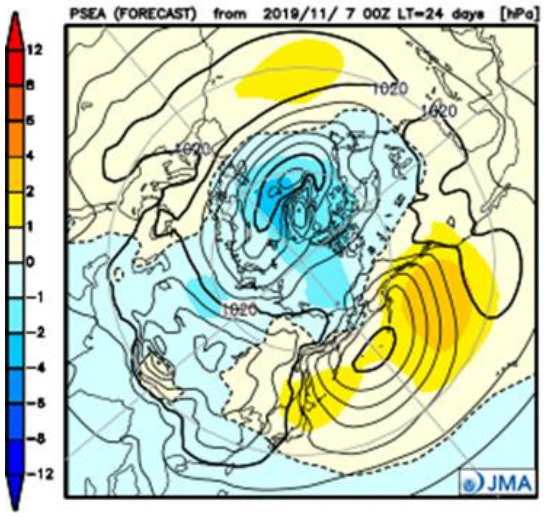

Figures 3-3 Predicted atmospheric fields from 20°N – 90°N for December–February 2019/2020 (ensemble mean of 51 members)
(a) Geopotential height at 500 hPa (contours) and anomaly (shading). The contour interval is 60 m.
(b) Sea level pressure (contours) and anomaly (shading). The contour interval is 4 hPa.

(Takuya Komori, Tokyo Climate Center)

JMA's Seasonal Ensemble Prediction System

JMA operates a seasonal Ensemble Prediction System (EPS) using the Coupled atmosphere-ocean General Circulation Model (CGCM) to make seasonal predictions beyond a one-month time range. The EPS produces perturbed initial conditions by means of a combination of the initial perturbation method and the lagged average forecasting (LAF) method. The prediction is made using 51 members from the latest four initial dates (13 members are run every 5 days). Details of the prediction system and verification maps based on 30-year hindcast experiments (1981–2010) are available at https://ds.data.jma.go.jp/tcc/tcc/products/model/.

<<Table of contents <Top of this article

Cold Season Outlook for Winter 2019/2020 in Japan

JMA issued its outlook for the coming winter (December 2019 – February 2020) over Japan in September and updated it in November based on the Agency's seasonal Ensemble Prediction System (EPS). This article outlines the outlook update of 25 November.

1. Outlook summary (Figure 4-1)

- Seasonal mean temperatures are expected to exhibit above-normal tendencies nationwide.
- Seasonal precipitation amounts on the Sea of Japan side of northern and eastern Japan, and seasonal snowfall amounts on the Sea of Japan side from northern to western Japan, are expected to exhibit below-normal tendencies.

2. Outlook background

Figure 4-2 highlights expected large-scale oceanic/atmospheric characteristics for winter. An outline of the background to the outlook is given below.

- ENSO-neutral conditions are likely to continue until winter. Sea surface temperatures (SSTs) are expected to be above normal over the western Indian Ocean and the western-central part of the tropical Pacific.
- In association with the expected SST anomalies, convection in the tropics is expected to be enhanced over the western Indian Ocean and the western-central Pacific and suppressed around the Indonesia.
- In the upper circulation fields, wave train conditions are expected to appear in association with the above-mentioned convective activity along the subtropical jet stream from the Eurasian continent to Japan with northward meandering around the latter, suggesting a weaker-than-normal winter monsoon.
- Tropospheric temperatures are expected to be above normal mainly due to the recent warming trend, which is likely to reduce the probability of below-normal temperatures.

(Hiroshi Ohno, Tokyo Climate Center)

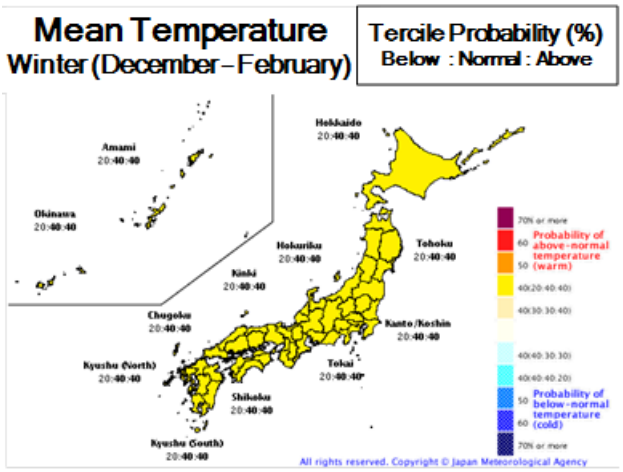

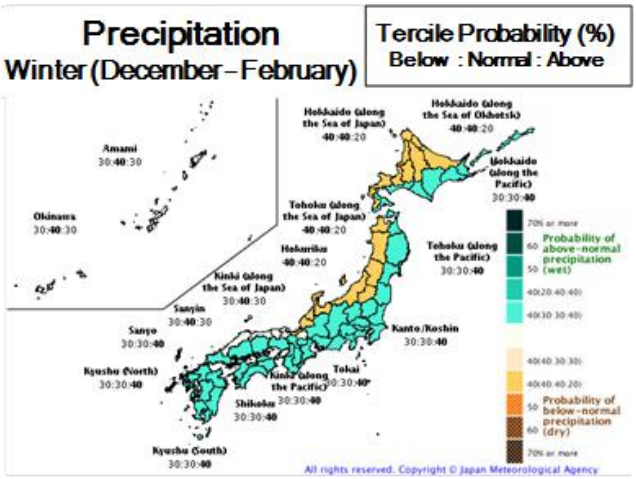

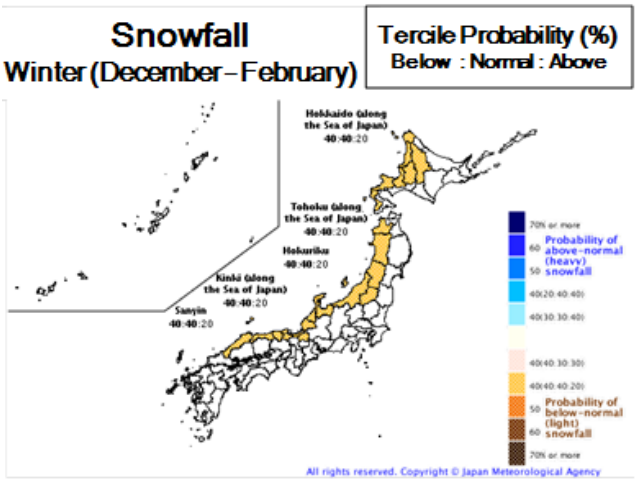

Figure 4-1 Outlook for winter 2019/2020 temperature (upper left), precipitation (upper right) and snowfall (lower left) probability in Japan.
Snowfall amounts are forecasted only for the Sea of Japan side from northern to western Japan.

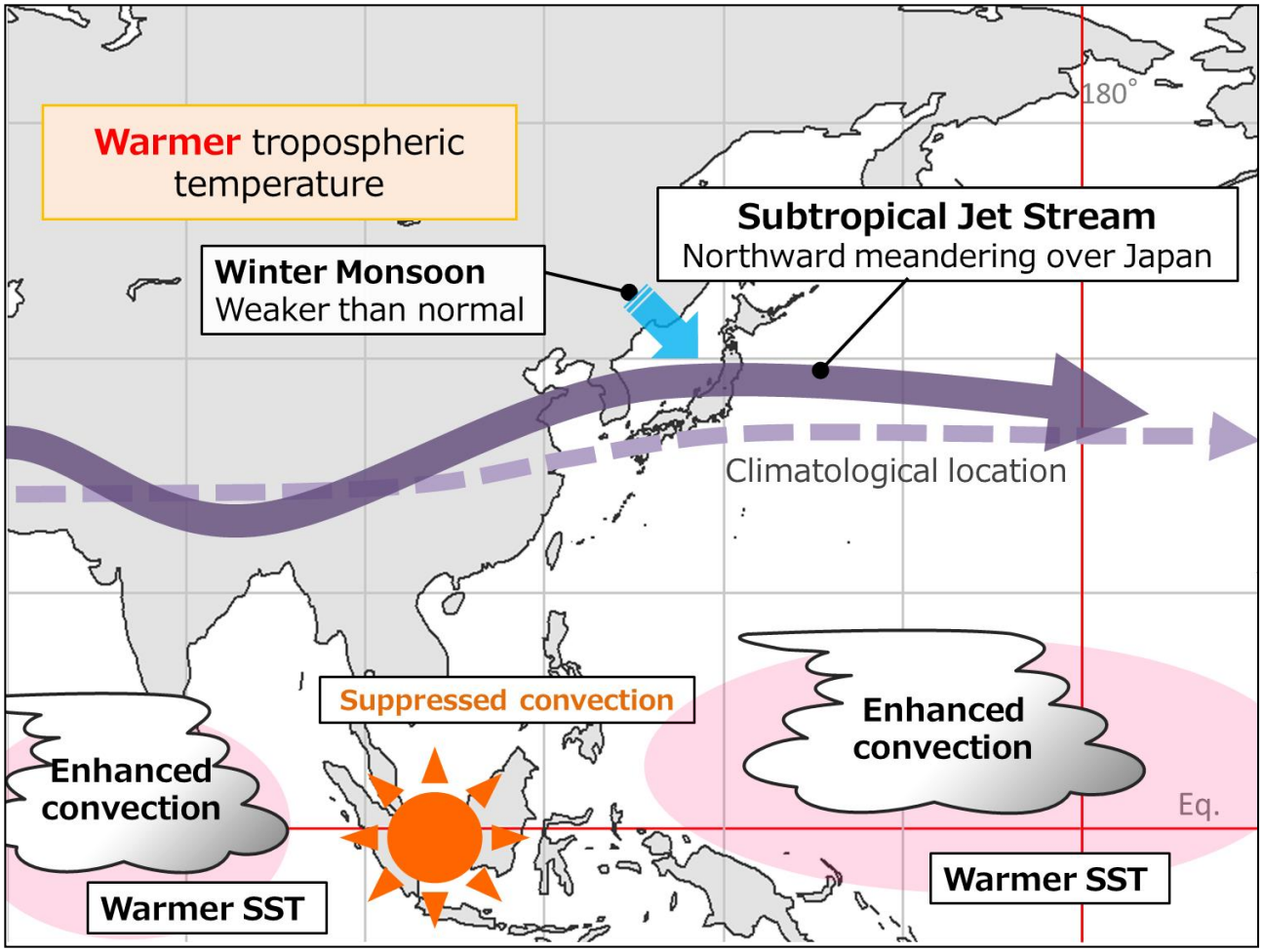

Figure 4-2: Conceptual diagram showing expected large-scale ocean/atmosphere characteristics for winter 2019/2020

<<Table of contents <Top of this article

Summary of the 2019 Asian Summer Monsoon

1. Precipitation and temperature

CLIMAT report data detailing four-month total precipitation amounts for the monsoon season (June – September) show more than 140% of the normal from the southern part of Central Asia to the central part of South Asia and in/around northern and northeastern China, while values less than 60% of the normal were seen in and around Indonesia, southern Pakistan and northwestern China, and from eastern China to the Korean Peninsula (Figure 5-1). In and around South Asia, heavy rain caused more than 1,900 fatalities from July to August (sources: governments of India/Pakistan, European Commission) and more than 360 in September (sources: government of India, European Commission). In Singapore, monthly precipitation in September was at its lowest for the month since 1869 according to the Meteorological Service Singapore.

Four-month mean temperatures for the same period were above normal in many parts of Asia. Anomalies of more than 1°C above normal were seen from northern China to the southern part of Central Siberia, from eastern China to northern Japan, and in and around southern China and southern Pakistan (Figure 5-2).

2. Tropical cyclones

A total of 18 tropical cyclones (TCs[1]) had formed over the western North Pacific and the South China Sea by September 2019, as compared to the normal of 18.4 (Table 5-1). From June to September, a total of 16 TCs (climatological normal: 16.0) formed, with 14 approaching or making landfall on East Asia and 11 (climatological normal: 9.2) on Japan.

Among these, Typhoon Lekima passed by Japan's Sakishima Islands with a maximum wind speed of 105 knots and made landfall on eastern China, resulting in more than 40 fatalities in the eastern part of the country (source: government of China).

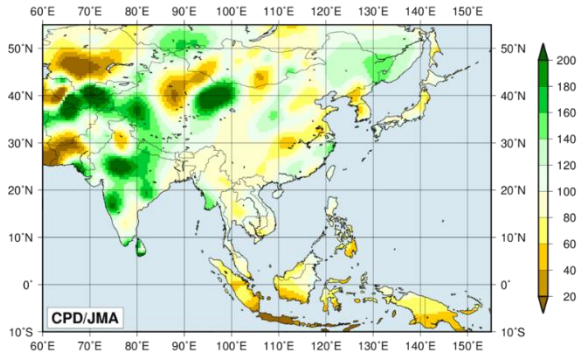

Figure 5-1 Four-month precipitation ratios (%) from June to September 2019

The base period for normal is 1981 – 2010. Note that the data in Afghanistan, Bhutan, Cambodia, Kazakhstan, Laos, Nepal, Papua New Guinea and Viet Nam are interpolated due to the lack of CLIMAT report or climatological normal.

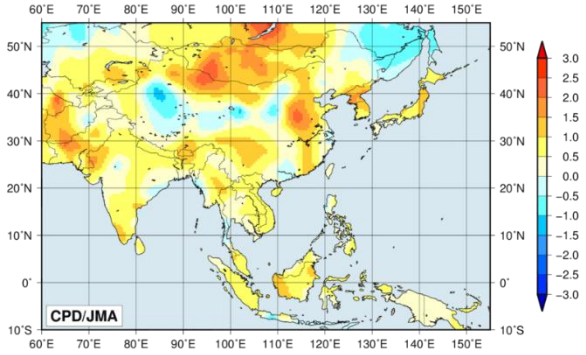

Figure 5-2 Four-month mean temperature anomalies (°C) from June to September 2019

The base period for normal is 1981 – 2010. Note that the data in Afghanistan, Bhutan, Cambodia, Kazakhstan, Laos, Nepal, Papua New Guinea and Viet Nam are interpolated due to the lack of CLIMAT report or climatological normal.

Table 5-1 Tropical cyclones forming over the western North Pacific up to September 2019

Number ID	Name	Date (UTC)	Category[1)]	Maximum wind[2)] (knots)
T1901	PABUK	1/1-1/4	TS	45
T1902	WUTIP	2/19-2/28	TY	105
T1903	SEPAT	6/27-6/28	TS	40
T1904	MUN	7/2-7/4	TS	35
T1905	DANAS	7/16-7/20	TS	45
T1906	NARI	7/25-7/27	TS	35
T1907	WIPHA	7/30-8/3	TS	45
T1908	FRANCISCO	8/2-8/6	TY	70
T1909	LEKIMA	8/4-8/12	TY	105
T1910	KROSA	8/6-8/16	TY	75
T1911	BAILU	8/21-8/25	STS	50
T1912	PODUL	8/28-8/29	TS	40
T1913	LINGLING	9/2-9/7	TY	95
T1914	KAJIKI	9/2-9/3	TS	35
T1915	FAXAI	9/4-9/9	TY	85
T1916	PEIPAH	9/15-9/16	TS	35
T1917[3)]	TAPAH	9/19-9/22	TY	65
T1918[3)]	MITAG	9/28-10/3	TY	75

Note: Based on information from the RSMC Tokyo-Typhoon Center.

1) Intensity classification for tropical cyclones.
TS: tropical storm,
STS: severe tropical storm,
TY: typhoon

2) Estimated maximum 10-minute mean wind.

3) Based on early analysis data, but not best track.

[1] Here, a TC is defined as a tropical cyclone with a maximum sustained wind speed of 34 knots or more.

3. Monsoon activity and atmospheric circulation

Convective activity (inferred from OLR) averaged for June – September 2019 was enhanced in and around the western Indian Ocean and over the sea northeast of the Philippines, while values were suppressed from the southeastern tropical Indian Ocean to the Maritime Continent and in/around the northwestern part of Southeast Asia (Figure 5-3). OLR index data (Table 5-2) indicate that the overall activity of the Asian summer monsoon (represented by the SAMOI (A) index) was below normal except in August. The active convection area was shifted northward of its normal position other than in June and October (SAMOI (N) index) and eastward other than in August and October (SAMOI (W) index). Convective activity over India and the Bay of Bengal (Figure 5-4 (a)) was suppressed from May to July and enhanced from August to September. Convective activity over the Philippines (Figure 5-4 (b)) was suppressed from mid-May to June and from late September to October, and was enhanced from August to mid-September.

In the upper troposphere (Figure 5-5 (a)), the northwestward extension of the Tibetan High was stronger than normal and anti-cyclonic circulation anomalies straddling the equator were seen from Africa to the western Indian Ocean. Such anomalies were also seen over the western tropical North Pacific. In the lower troposphere (Figure 5-5 (b)), cyclonic circulation anomalies were seen over and around the Arabian Sea and over the southern part of the East China Sea, while anti-cyclonic circulation anomalies straddling the equator were seen over the eastern Indian Ocean. The monsoon trough over Southeast Asia was shifted northeastward of its normal position, and surface westerly winds were weaker than normal over the Bay of Bengal (Figure 5-6). Zonal wind shear between the upper and lower troposphere over the northern Indian Ocean and southern Asia (Figure 5-7) was weaker than normal from May to early June and from late September to mid-October.

(Hitoshi Sato, Tokyo Climate Center)

References

Wang, B. and Z. Fan, 1999: Choice of South Asian summer monsoon indices. *Bull. Amer. Meteor. Soc.*, **80**, 629–638.

Webster, P. J. and S. Yang, 1992: Monsoon and ENSO: Selectively interactive systems. *Quart. J. Roy. Meteor. Soc.*, **118**, 877 – 926.

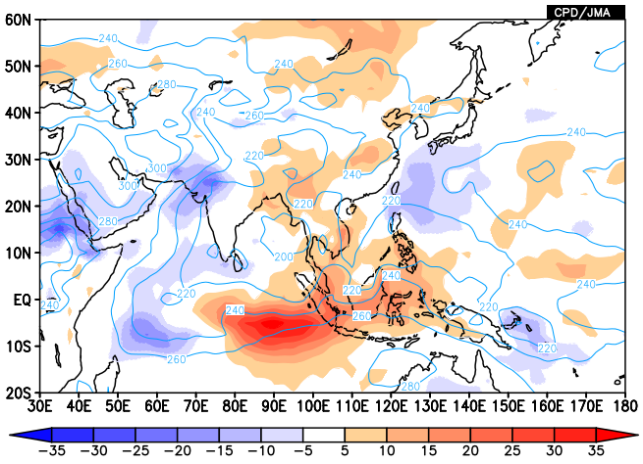

Figure 5-3 Four-month mean OLR and its anomaly (W/m^2) for June–September 2019
The contours indicate OLR at intervals of 20 W/m^2, and the color shading denotes OLR anomalies from the normal (i.e., the 1981–2010 average). Negative (cold color) and positive (warm color) OLR anomalies show enhanced and suppressed convection compared to the normal, respectively. Original data are provided by NOAA.

Table 5-2 Summer Asian Monsoon OLR Index (SAMOI) values observed from May to October 2019
Asian summer monsoon OLR indices (SAMOI) are derived from OLR anomalies from May to October. SAMOI (A), (N) and (W) indicate the overall activity of the Asian summer monsoon, its northward shift and its westward shift, respectively. SAMOI definitions are as follows: SAMOI (A) = (-1) × (W + E); SAMOI (N) = S – N; SAMOI (W) = E – W. W, E, N and S indicate area-averaged OLR anomalies for the respective regions shown in the figure on the right normalized by their standard deviations.

	Summer Asian Monsoon OLR Index (SAMOI)		
	SAMOI (A): Activity	SAMOI (N): Northward-shift	SAMOI (W): Westward-shift
May 2019	-1.8	+1.8	-1.1
Jun. 2019	-0.8	-1.5	-0.1
Jul. 2019	-1.1	+1.4	-1.3
Aug. 2019	+0.4	+0.8	0.0
Sep. 2019	-0.9	+2.8	-0.2
Oct. 2019	-1.7	-0.8	+0.8

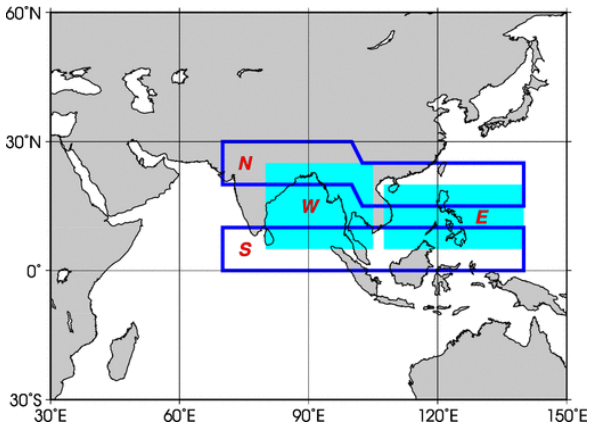

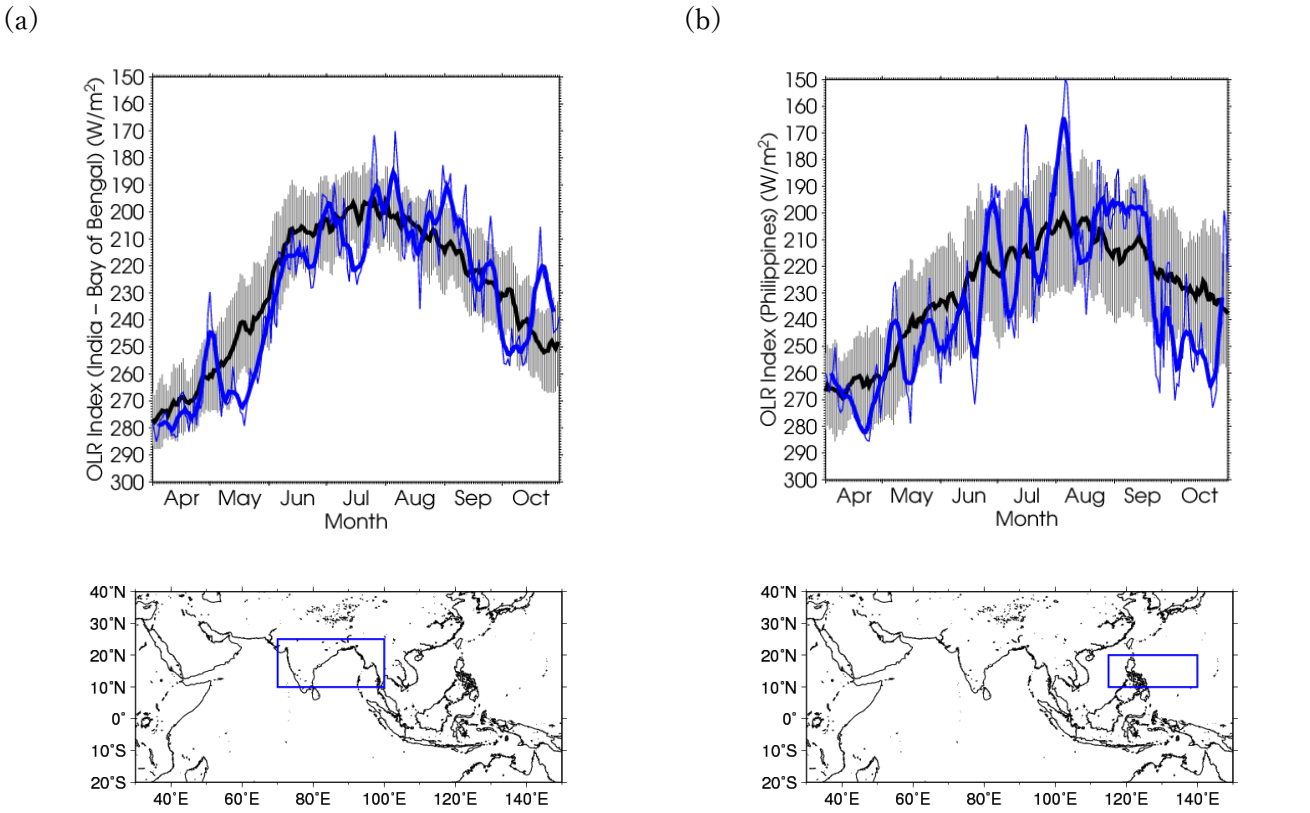

Figure 5-4 Time-series representation of OLR (W/m^2) averaged over (a) India and the Bay of Bengal (shown by the rectangle on the bottom: 10°N - 25°N, 70°E - 100°E) and (b) the Philippines (shown by the rectangle on the bottom: 10°N - 20°N, 115°E - 140°E)

The OLR indices are calculated after Wang and Fan (1999). The thick and thin blue lines indicate seven-day running mean and daily mean values, respectively. The black line denotes the normal (i.e., the 1981 - 2010 average), and the gray shading shows the range of the standard deviation calculated for the time period of the normal.

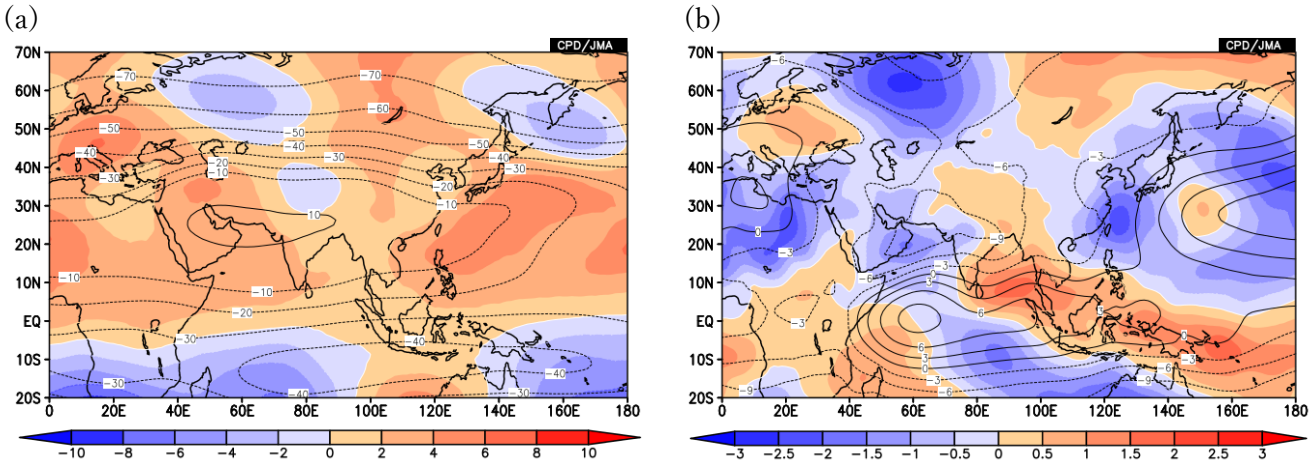

Figure 5-5 Four-month mean (a) 200-hPa and (b) 850-hPa stream function (contour) and its anomaly (color shading) (10^6 m^2/s) for June–September 2019

Contour intervals are (a) 10 × 10^6 m^2/s and (b) 3 × 10^6 m^2/s. Warm (cold) shading denotes anti-cyclonic (cyclonic) circulation anomalies in the Northern Hemisphere, and vice-versa in the Southern Hemisphere. The base period for the normal is 1981 – 2010.

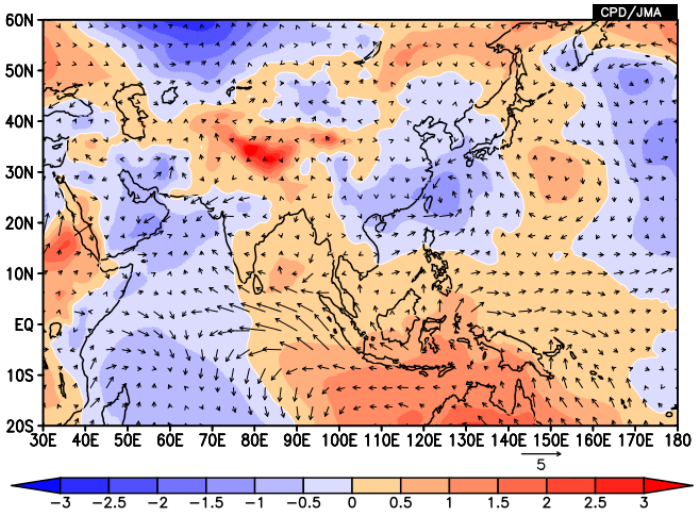

Figure 5-6 Sea level pressure anomaly (color shading) (hPa) and surface wind vector anomaly (vectors) (m/s) for June–September 2019.
The shading shows sea level pressure anomalies at intervals of 0.5 hPa. The base period for the normal is 1981 – 2010.

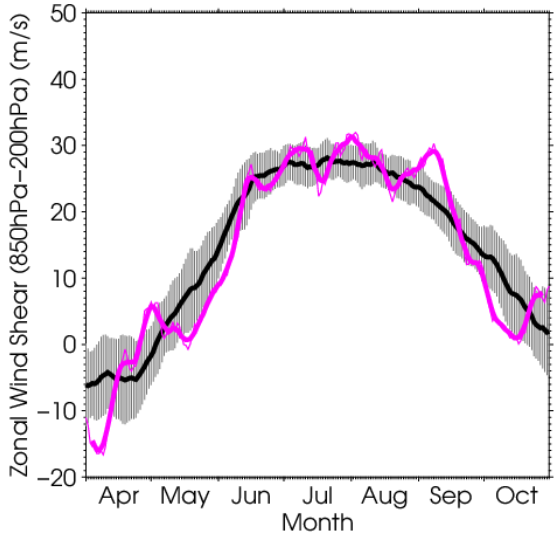

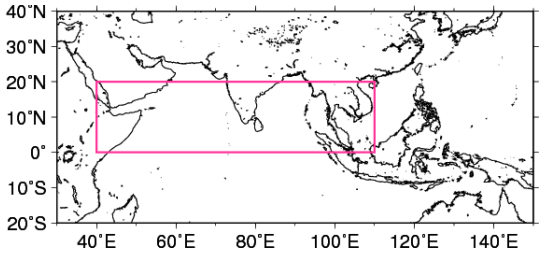

Figure 5-7 Time-series representation of the zonal wind shear index between 200-hPa and 850-hPa averaged over the northern Indian Ocean and southern Asia (the region enclosed by the pink rectangle in the right figure: equator – 20°N, 40°E – 110°E)
The zonal wind shear index is calculated after Webster and Yang (1992). The thick and thin pink lines indicate seven-day running mean and daily mean values, respectively. The black line denotes the normal (i.e., the 1981 – 2010 average), and the gray shading shows the range of the standard deviation calculated for the time period of the normal.

<<Table of contents <Top of this article

Status of the Antarctic Ozone Hole in 2019

The Antarctic ozone hole in 2019 was at its smallest since 1990.

Since the early 1980s, the Antarctic ozone hole has appeared every year in austral spring with a peak in September or early October. It is generally defined as the area in which the total ozone column value is below 220 m atm-cm.

JMA analysis based on data from the Ozone Monitoring Instrument (OMI) on the Aura platform indicates that the Antarctic ozone hole in 2019 appeared in mid-August and expanded before unexpectedly peaking in size in 7 September, remaining under 11.0 million square kilometers in scale (0.8 times the size of the Antarctic Continent) until its disappearance on 10 November (Figure 6-1).

This significantly reduced scale can be mainly attributed to the particular meteorological conditions of 2019, including stratospheric temperatures that were much higher than the most recent decadal average after August. This hindered the formation of polar stratospheric clouds (PSCs), which play an important role in ozone destruction. In addition, a weak polar vortex induced flows of high-concentration ozone from low latitudes.

As an overall trend, the maximum size of the Antarctic ozone hole has shown a statistically significant decrease since 2000. *The WMO/UNEP Scientific Assessment of Ozone Depletion: 2018 report* detailed how the hole is expected to close gradually, with springtime total column ozone in the 2060s returning to 1980 values.

The ozone layer acts as a shield against ultraviolet radiation, which can cause skin cancer. The ozone hole was first recognized in the early 1980s, and large-scale events have been observed since the 1990s. Its record size was 29.6 million square kilometers (2000). The Antarctic ozone hole significantly affects summer climatic conditions on the surface of the Southern Hemisphere according to the recent assessment.

(Mika Kimura, Ozone Layer Monitoring Center)

<<Table of contents <Top of this article

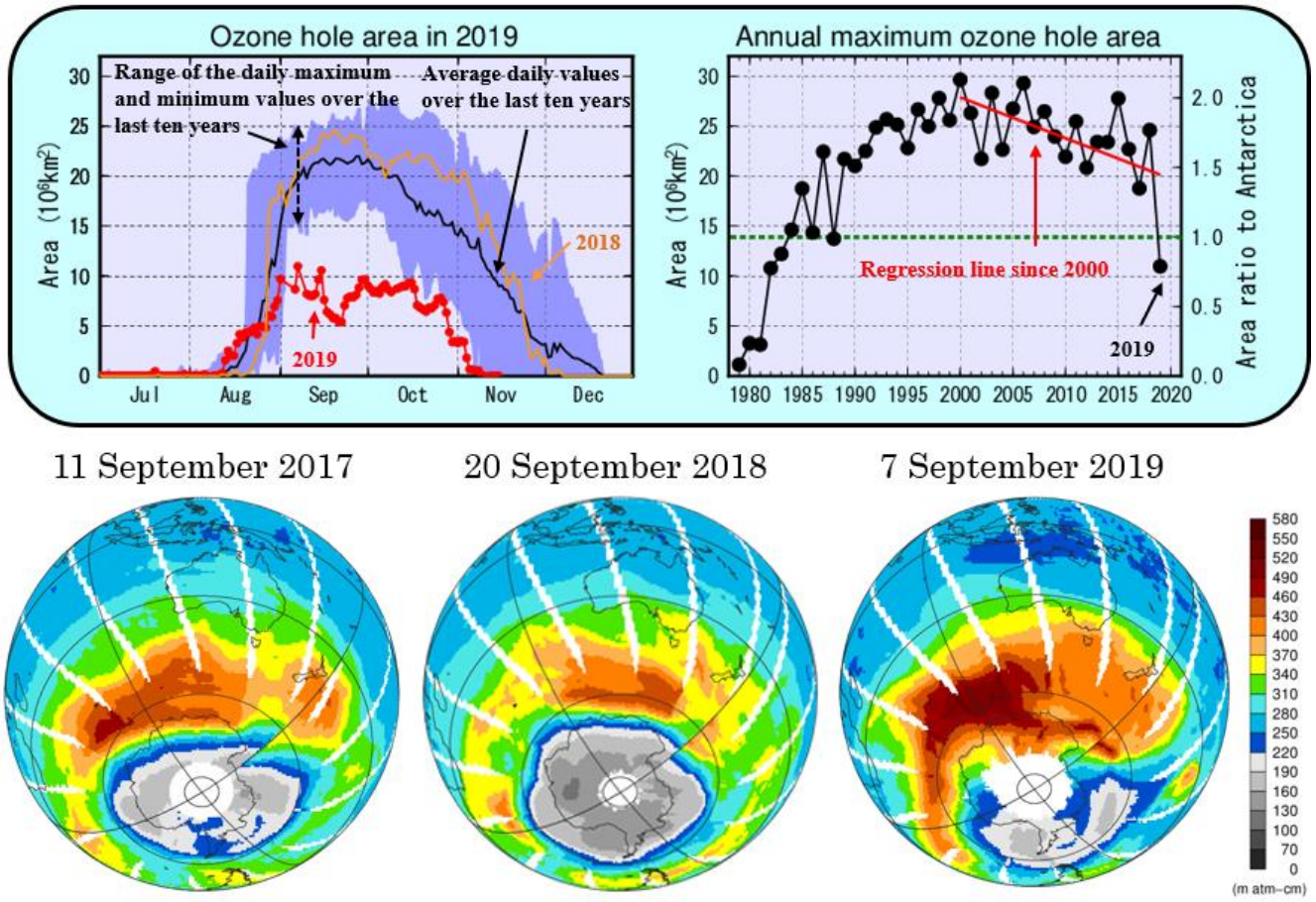

Figure 6-1 Characteristics of the Antarctic ozone hole
Upper left: Time-series representation of the daily ozone hole area for 2019 (red line) and the 2009–2018 average (black line). The blue shading area represents the range of daily minima and maxima over the past 10 years.
Upper right: Inter-annual variability of annual maximum ozone hole area. The green dotted line shows the area of the Antarctic Continent (13.9 million square kilometers).
Bottom: Snapshots of total column ozone distribution on the day of the annual maximum ozone hole area for the last three years; the ozone hole is shown in gray (below 220m atm-cm). These panels are based on data from NASA satellite sensors of the Ozone Monitoring Instrument (OMI).

TCC contributions to Regional Climate Outlook Forums

WMO Regional Climate Outlook Forums (RCOFs) bring together national, regional and international climate experts on an operational basis to produce regional climate outlooks based on input from participating NMHSs, regional institutions, Regional Climate Centres and global producers of climate predictions. By providing a platform for countries with similar climatological characteristics to discuss related matters, these forums ensure consistency in terms of access to and interpretation of climate information.

In autumn 2019, TCC dispatched experts to SASCOF-15, and EASCOF-7.

SASCOF-15

India Meteorological Department (IMD) hosted the 15th winter session of the South Asian Climate Outlook Forum (SASCOF-15) from 23 to 25 September 2019 in Thiruvananthapuram, Kerala, India. The event was supported by the World Meteorological Organization (WMO), the Regional Climate Centre (RCC) Pune of the IMD, the UK Met Office (UKMO) and the Regional Integrated Multi-hazard Early-warning System for Africa and Asia (RIMES) with funding from the Asia – Regional Resilience to Changing Climate (ARRCC) program based on UKMO and RIMES collaboration. More than 40 attendees discussed climatic conditions during the upcoming winter monsoon season (Oct. to Dec. 2019) and effective use of climate services in user sectors.

As part of the activities of WMO's Regional Climate Centre, and also as Global Producing Center for long-range forecasts (GPC-LRF), two experts from Tokyo Climate Center provided an introduction of TCC and a winter monsoon season outlook. The outlook was based on JMA's dynamical seasonal ensemble prediction system with probabilistic information on atmospheric variability and the evolution of oceanic conditions in the tropical Pacific and Indian Ocean for the period from Oct. to Dec. 2019. The provision of this information was intended to support the output of country-scale outlooks by National Meteorological and Hydrological Services (NMHSs) in South Asia and contribute to the summarization of a consensus outlook for South Asia.

The forum placed particular emphasis on the Climate Services User Forum (CSUF) with focus on the water sector based on the sharing of information with user sectors to support discussion of their experiences of using climatic services. The TCC experts were also involved in active discussions to promote better use of climate services through future SASCOF activities.

EASCOF-7

The seventh session of EASCOF (EASCOF-7), hosted by the National Agency for Meteorology and Environmental Monitoring (NAMEM), was held in Ulaanbaatar in Mongolia from 5 to 7 November 2019. More than 40 experts from China, Japan, the Republic of Korea and Mongolia attended to discuss the characteristics of summer 2019, which exhibited significant intra-seasonal variations, and the seasonal forecast for the winter monsoon in East Asia. Discussions also covered recent understandings on climate variations in the East Asian monsoon. Two TCC experts each gave presentations at the forum on 1. the high precipitation levels and late onset/end of the summer 2019 rainy period in East Asia, and 2. the outlooks for El Niño and the coming winter. Exchanges of expertise at this three-day forum are expected to help develop attendees' understanding of phenomena related to the East Asian monsoon and support improvement of their climate services.

SASCOF-15

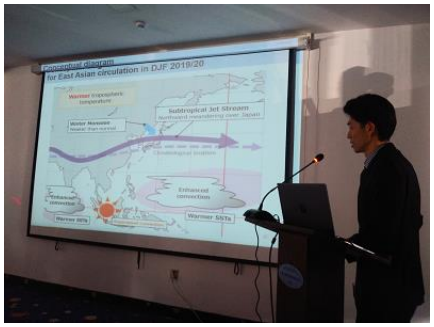

EASCOF-7

(SASCOF-15: Kazuaki Tsuji, Tokyo Climate Center, EASCOF-7: Shoji Notsuhara, Tokyo Climate Center)

<<Table of contents <Top of this article

You can also find the latest newsletter from Japan International Cooperation Agency (JICA).
JICA's World (October 2019)
https://www.jica.go.jp/english/publications/j-world/1910.html
JICA's World is the quarterly magazine published by JICA. It introduces various cooperation projects and partners along with the featured theme. The latest issue features "Climate Actions: For the Future of the Planet".

Any comments or inquiry on this newsletter and/or the TCC website would be much appreciated. Please e-mail to tcc@met.kishou.go.jp.
(Editors: Yasushi Takatsuki, Yasushi Mochizuki and Kazuaki Tsuji)

Tokyo Climate Center (TCC), Japan Meteorological Agency
Address: 1-3-4 Otemachi, Chiyoda-ku, Tokyo 100-8122, Japan

TCC Website: https://ds.data.jma.go.jp/tcc/tcc/index.html